A REGION-BASED APPROACH FOR DESCRIBING URBAN MORPHOLOGY BASED ON SUB-PIXEL ESTIMATION OF SEALED SURFACE COVER

T. Van de Voorde [a, *], W. Jacquet [b c], F. Canters [a]

[a] Dept. of Geography, Cartography and GIS Research Group, Vrije Universiteit Brussel, Pleinlaan 2, 1050 Brussels, Belgium - (tvdvoord, fcanters)@vub.ac.be

[b] Dept. of Mathematics, Vrije Universiteit Brussel , Pleinlaan 2, 1050 Brussels, Belgium – wolfgang.jacquet@vub.ac.be

[c] Dept. of Physics, Vision Lab IBBT, University of Antwerp, Universiteitsplein 1, 2610 Wilrijk, Belgium

KEY WORDS: Urban remote sensing, Urban morphology, Land use, Spatial metrics, Greater Dublin Area

ABSTRACT:

Earth observation provides regular information on urban development and could provide an important contribution to map and monitor structural characteristics of expanding cities. While most contemporary remote sensing research in urban environments tends to focus on high resolution satellite imagery, urban monitoring and modelling applications usually rely on extensive historic archives of landuse maps with a large geographic extent. Medium resolution images therefore seem better suited for these applications. Their lower resolution, however, inhibits studying urban morphology and change processes at an intra-urban level. In this research, we circumvent that problem by developing spatial metrics for use on continuous sealed surface data produced by sub-pixel classification of Landsat ETM+ imagery covering the city of Dublin, Ireland. Metrics we developed are based on the shape of the cumulative frequency distribution of estimated sub-pixel fractions at block level, as well as on spatial variation of sub-pixel fractions within each urban block. A MLP classifier is then used to relate the metric variables to urban landuse classes selected from the MOLAND topology. In combination with density information derived from the sealed surface maps, our approach allows producing maps describing urban morphology and intra-urban dynamics. These maps are a valuable source of information to aid the calibration of land-use change models.

1. INTRODUCTION

More than half of the earth's inhabitants reside in urban areas and their share in the global population is still increasing (Martine, 2007). While spatial expansion of cities is a natural consequence of demographic trends on which local and regional policy-makers have little grasp, local policy should consider how population growth is translated into spatial patterns of urban growth. Urban sprawl and increased soil sealing provide symptomatic evidence for the fact that many European and North-American cities grow faster spatially than demographically. A study of the European Environment Agency confirms this and reports that European cities have expanded on average by 78% since the mid-1950s, while during the same period population increased by only 33% (EEA, 2006). Effective urban management and planning strategies are therefore essential to temper the consequences of urban land consumption on the natural and human environment. To develop and monitor such strategies and to assess their spatial impact, analysing and characterising changes in urban structure is of great consequence. Data from earth observation satellites provide regular information on urban development and could in that way contribute to mapping and monitoring structural characteristics of expanding cities. A rather novel approach in this research area is to describe urban form by means of spatial metrics, i.e. quantitative measures of spatial pattern and composition which have recently shown considerable potential for structural analysis of urban environments (Herold et al., 2005). Spatial metrics derived from satellite imagery may help to describe the morphological characteristics of urban areas and their changes through time (Ji et al., 2006). However, because high resolution satellite imagery is only available since around 2000, historic image archives mostly consist of medium resolution (MR) data such as from the Landsat or SPOT programmes. Such images are cheap, widely available and offer a wealth of information that may be useful for urban monitoring purposes at strategic planning levels, especially when a historic perspective of 10 years or more is required. On the other hand, the lower resolution of these data makes them more suited for small-scale studies at city-level or at the level of large administrative units or counties and less suited for intra-urban analysis. This is because many details on intra-urban structure and composition are lost due to the occurrence of different scene elements within the pixel (Cracknell, 1998). Spectral unmixing approaches, which allow characterising land-cover distribution at sub-pixel level, may partly compensate for this lack of spatial detail, and may render medium-resolution imagery more useful for urban studies (Rashed et al., 2001). In an urban context, these approaches are frequently used to map sealed surface cover (Weng, 2008), an important structural element of urban areas.

The main objective of this paper is to examine the possibilities of using MR satellite images for characterising intra-urban spatial structure. Previous studies have either used spatially more detailed data or have treated cities at more coarse levels of analysis. Because of this, they usually applied patch or landscape-based spatial metrics on discrete, categorical land-cover maps. Our aim in the present study is to characterise intra-urban morphology with newly developed region-based spatial metrics calculated on a continuous sealed surface map derived from MR satellite imagery through spectral unmixing. In a second step, the structural characteristics captured by these metrics are used as variables in a supervised classification approach in order to establish a link between urban morphology and broadly defined land-use types. The result is a land-use map reflecting both urban density and functional characteristics of

* Corresponding author.

the urban fabric at the time of image acquisition. The method is applied on the city of Dublin, Ireland using 30m resolution Landsat ETM+ imagery. The approach can easily be repeated for each image in a time-series to analyse changes in urban structure. It may therefore add value to the extensive historic archives of MR images by characterising urban growth patterns at a reasonably detailed level and on an intra-urban basis.

2. DATA AND SCALE OF ANALYSIS

The study area for this research is Dublin, the political and economic capital of Ireland and home to over 40% of the country's population. A Landsat TM image (path 206, row 23) acquired on May 24th 2001 was used for characterising the urban morphology of the study area. The image was geometrically co-registered to the Irish Grid projection system and the raw digital numbers were converted to exoatmospheric reflectance according to the formulas and calibration parameters presented by The Landsat 7 Users Handbook (Irish, 2007). An existing land-cover map, derived from a 1m pan-sharpened Quickbird image acquired on August 4th 2003, was used to obtain reference data for training and validating the sub-pixel classifier. Reference land-use classes were acquired from the European MOLAND land-use map of Dublin for the year 2000.
Spatial metrics are calculated within a spatial domain, i.e. a relatively homogeneous spatial entity that represents a basic landscape element. Naturally, the definition of the spatial domain directly influences the metrics and will depend on the aims of the study and the characteristics of the landscape (Herold, et al., 2005). In this study, the basic entities of analysis were defined by intersecting detailed urban road network data for Dublin with the MOLAND land-use map of 2000. This provided us with a large number of blocks that are relatively homogeneous in terms of land use. Given the resolution of the image data, blocks smaller than 1 ha. (corresponding to approximately 11 pixels) were topologically removed. The threshold of 1ha. corresponds to the minimum mapping unit employed for urban areas within the MOLAND dataset. In all, 5767 spatial units were used in the analysis.

3. METHODS

3.1 Deriving a sealed surface map by spectral mixture analysis

One of the most commonly used methods for deriving sub-pixel sealed surface fractions is LSMA, linear spectral mixture analysis (e.g. Ward, et al., 2000). In this approach, a pixel's observed reflectance is modelled as a linear combination of spectrally pure "endmember" reflectances (van der Meer, 1999). The advantage of LSMA is that it is a physically based model that does not require extensive training data, but only the definition of end-member signatures. Applying LSMA effectively, however, requires that the endmembers can be defined unambiguously and that they can be related to meaningful land-cover types. This is often not the case in multispectral data of urban areas because of spectral confusion between artificial sealed surface and non-urban surface types such as bare soil (Van de Voorde et al., 2009). In studies where fractions of only a single land-cover class are required, linear or non-linear regression analysis provides an interesting alternative for unmixing. Several authors have successfully applied bi-variate or multiple regression to relate sub-pixel impervious surface or vegetation cover as a dependent variable to the spectral values of Landsat pixels or derivatives thereof (e.g. Bauer et al., 2008). Yet also in this case, obtaining accurate sealed surface fractions in the presence of spectrally similar non-urban land-cover types within the scene remains problematic. To circumvent this problem, we first developed a mask identifying pixels that belong to the urban area with an unsupervised classification approach. The resulting map was subsequently enhanced by a knowledge-based post-classification approach (Van de Voorde et al., 2007). The final classification consisted of 4 classes: urban areas including mixed sealed surface/vegetation pixels, pure vegetation pixels (e.g. trees, crops, pasture), bare soil and water. Validation was carried out by a visual sampling of about 1% of the image pixels (2897 pixels). Pixels belonging to the classes soil, water and pure vegetation were considered to have zero sealed surface cover. Pixels within the bounds of the area belonging to the urban class were considered as mixtures of sealed surfaces and vegetation, and they were therefore subjected to sub-pixel analysis. Because sub-pixel fractions are required for just a single end-member, we decided to apply a stepwise multiple regression with the vegetation fraction as independent variable, assuming that within the urban area the fraction of sealed surfaces is the complement of the vegetation fraction. A map with sealed surface proportions could then be derived by subtracting the vegetation fraction from one. To define the regression model and for validating it, an initial sample of approximately 10 000 pixels was randomly drawn from the part of the Landsat image overlapping the already available high resolution land-cover map, which was downsampled to 30m resolution for calculating reference proportions of vegetation cover. Pixels in the sample that underwent changes in vegetation cover between the acquisition dates of the Landsat image and the Quickbird image used to derive the land-cover map were filtered out by a temporal filtering technique based on iterative linear regression between NDVI values (Van de Voorde et al, 2009). From the unchanged sample pixels coinciding with the urban mask, a random sample of 2500 training and 2500 validation pixels was finally selected. The accuracy of sealed surface proportions was assessed for the validation sample with two error measures. The mean absolute error of the sealed surface fraction (MAESealed) was used as a measure of the error magnitude. It is calculated as the mean across the validation sample of the absolute differences between sealed surface fractions predicted by the regression model and the corresponding reference proprortions derived from the ground truth. In addition, the mean error (MESealed) was calculated without using absolute values for the difference between predicted and reference proportions. It was used to indicate a possible bias in the proportion estimates (over or underestimation).

3.2 Characterising urban morphology within predefined spatial units

A simple approach to relate the sub-pixel sealed surface proportions within a spatial entity (block) to urban morphology is by calculating the fraction of sealed surface cover for each block, i.e. the mean of the per-pixel sealed surface fractions. This provides a variable that expresses built-up density at block level. With this variable, the study area was stratified into 4 urban density classes using criteria defined in the MOLAND typology: 0-10% (non-urban land), 10-50% (discontinuous sparse urban fabric), 50-80% (discontinuous urban fabric) and more than 80% (continuous urban fabric). Blocks with less than 10% sealed surfaces were directly labelled as non-urban land. Blocks with more than 80% sealed surface cover were

considered as continuous, dense urban fabric which could not be characterised further in terms of morphology. The remaining 3494 blocks with 10%-80% sealed surface cover were further analysed because they belong to morphological distinct land-use types such as sparse residential areas, industrial zones, etc. These could not be distinguished based on just the average sealed surface cover, which is only a general measure of composition that does not take spatial context into account. To describe the spatial pattern of sealed surface fractions within each block, we first calculated spatial variance (SV), a simple measure for spatially explicit characterisation of block morphology:

$$SV = \frac{\sum_{i}^{n}\sum_{j}^{k_i}(f_i - f_j)^2}{\sum_{i}^{n} k_i} \quad (1)$$

where

n = number of pixels with the block
k_i = number of neighbours of pixel i
f_i = subpixel sealed surface fraction

To further characterise the blocks, we also examined the cumulative frequency distribution (CFD) of the proportion sealed surface cover of the Landsat pixels within each block. Our assumption was that the shape of this distribution function should be related to the morphological characteristics of the block it represents. Low and medium density residential land-use blocks, for instance, contain more mixed sealed surface-vegetation pixels than industrial areas, which are mostly characterized by larger building structures. The abundance of these mixed pixels in the former, and the predominance of pure sealed surface pixels in the latter case should be reflected in the shape of the CFD. To express the CFD's shape quantitatively, a logistic function was fitted using a nonlinear least-squares approach. In its basic form a logistic function describing the relation between the cumulative frequency $P_i(f)$ of pixels with impervious surface fractions smaller than or equal to f occurring within a block i is given by:

$$P_i(f) = \frac{1}{1+e^{-f}} \quad (2)$$

The point of inflection for this function is 0.5 at a value for f of 0. To allow numerical fitting to CFD's of different shape, this basic logistic function was scaled and translated along the x and y axes:

$$P_i(f) = \gamma\frac{1}{1+e^{-(\alpha f+\beta)}} + \delta \quad (3)$$

where

α, γ = scaling parameters of the x and y axes
β, δ = translation parameters

In our analysis, we were only concerned with the part of the function domain and range that falls within the box defined by the interval $0 \le f \le 1$ and $0 \le P_i(f) \le 1$.
Although the fitted function is fully determined by its four parameters, semantically more meaningful and more easily interpretable descriptors of the function's shape may be derived. The position of the point of inflection $I\{Pi(f), f)\}$ is where the logistic curve changes from progressive to degressive growth, and can be determined from the second order derivative:

$$I_{\{P_i(f),f)\}} = \left(\frac{-\beta}{\alpha}; \frac{\gamma}{2} + \delta\right) \quad (4)$$

In case of a more "exponentially" shaped CFD, the point of inflection of the fitted curve lies outside the area of interest, i.e. the unit square. The offset of the function, or its intercept point with the y axis is a second useful characteristic and is given by:

$$O = \gamma\frac{1}{1+e^{-\beta}} + \delta \quad (5)$$

The offset takes on values closer to 1 in case pure vegetation pixels are present within the spatial unit.

3.3 Relating morphology to land use with MLP-based supervised classification

Together with the average fraction of sealed surfaces and the spatial variance of sealed surface fractions within the blocks, the 4 parameters of the fitted logistic curve were used as variables in a supervised classification. The primary objective was to assign each block with a sealed surface cover between 10% and 80% (3494 in total) to one of 5 urban land-use types corresponding to aggregates of classes in the MOLAND scheme: urban green (comprised of urban parks, sports and leisure facilities), residential areas, commercial areas, industrial zones and public or private services. The urban green class was included because some urban parks have more than 10% sealed surface cover due to the presence of walkways and small constructions. Blocks with more than 80% sealed surface cover were directly assigned to a sixth class: "continuous urban fabric". These blocks are too densely built to further characterise them based on the spatial distribution and the frequency distribution of constituent pixels with different sealed surface proportions. Likewise, pixels with 10% or less sealed surface cover were assigned to the class "non-urban land". To obtain reference data for training and validation of the classifier, the predominant land-use class of each block was derived from the MOLAND land-use map of 2000. Because the 5 target land-use classes are unevenly distributed, we adopted a stratified sampling approach to select training and validation samples. For each class, about 200 blocks were randomly selected. This set was then randomly split in two to obtain independent training and validation samples.
A multi-layer perceptron (MLP) classifier was then used to assign the blocks to the land-use classes. MLP is the most commonly used neural network classifier in remote sensing applications (Atkinson, 1997). Neural networks have gained popularity in the field because in contrast to statistical classifiers they are non parametric and therefore make no

assumptions about the frequency distribution of the sample data describing each class. This property is particularly interesting when variables with non-normal distributions are used for classification, as is the case in this research. After a satisfying classification result was obtained, the resulting land-use map was intersected with an urban density map that was derived by averaging the per-pixel sealed surface fractions within each block and dividing them into the 4 classes discussed earlier (< 10%, 10-50%, 50-80%, > 80%).

4. RESULTS AND DISCUSSION

4.1 Defining the urban area

The overall accuracy and kappa index of agreement of the initial classification used to delineate the urban area are 93% and 89% respectively. The highest errors were found for the bare soil class, which has a producer's accuracy of 68% and a user's accuracy of 88%. This error was mainly caused by confusion between bare soil and vegetation, which can be attributed to the mixed pixel problem (e.g. within agricultural fields or pastures). The fuzzy nature of these classes at 30 meter resolution even makes it difficult to assign them unambiguously to a single class during visual interpretation. For the purpose of deriving an urban mask, confusion between vegetation and bare soil posed no problem as both classes were considered to have no sealed surface cover. Misclassification of bare soil into urban areas occurred less frequently, and mostly at or near construction zones. An urban mask was derived by aggregating the classification result into two classes: urban and non-urban.

4.2 Sealed surface mapping

The stepwise linear regression analysis carried out on the training data resulted in 4 statistically significant linear models ($p < 0.05$). The normalised infrared band (band 4) was selected first because of its high correlation of 0.83 with the independent variable, i.e. proportional vegetation cover. This variable alone explains almost 70% of the observed variation in sub-pixel vegetation cover. Adding band 5 leads to a model with slightly higher explanatory capabilities and lower standard errors, but adding more variables leads to redundancy. From this analysis, the following model was selected and subsequently applied to the entire image:

$$V_j = -1.584 + 0.007\ B_4 + 0.006\ B_5 \qquad (6)$$

where

V_j = the estimated proportion of sub-pixel vegetation cover (0-1) for pixel i
B_4 = ETM+ band 4 (near infrared)
B_5 = ETM+ band 5 (short-wave infrared)

The sealed surface fractions estimated by equation (6) have a mean error of 0.0047 on the validation set consisting of 2500 pixels sampled within the urban mask, with a 95% confidence interval of [-0.008; 0.0103]. This constitutes a negligible positive bias which implies that overestimations of sealed surface cover within some sample pixels are compensated for by underestimations within others. The mean absolute error provides a more clear perspective on the error magnitude. Its value of 0.1048 with a 95% confidence interval of [0.1011; 0.1085] points to an average sub-pixel estimation error of about 10%. This is acceptable given the constraints put on the unmixing approach in terms of geometric co-registration, image noise and autocorrelation effects.

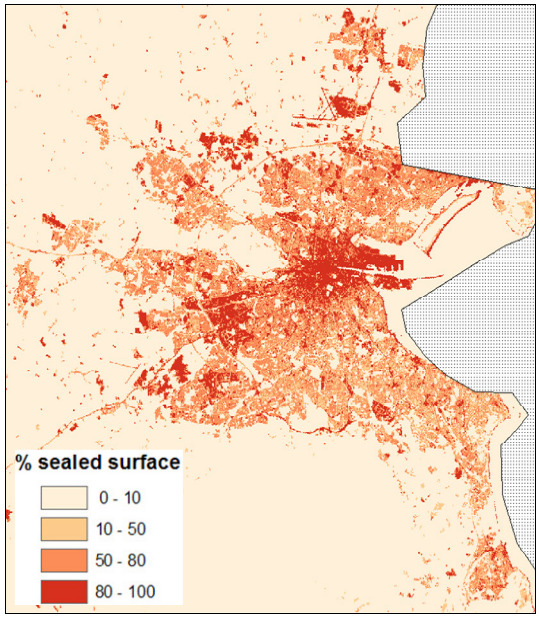

Figure 1 Sealed surface map, indicating the % sealed surface cover for each pixel

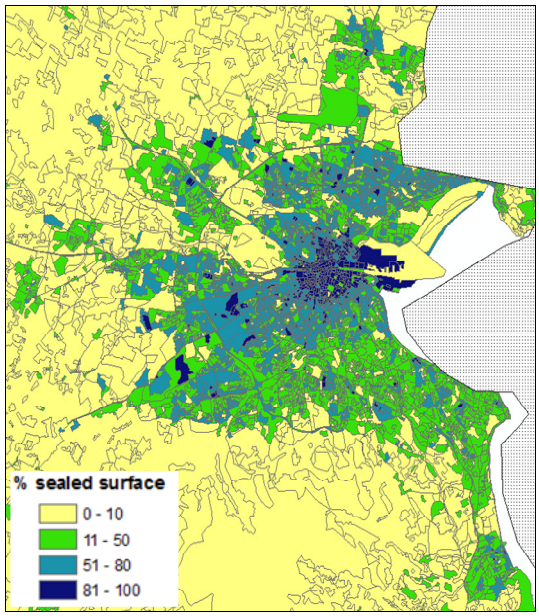

Figure 2 Urban density map indicating average sealed surface cover inside each urban block

Applying the regression model to all pixels that belong to the urban mask and setting all pixels outside the mask to zero provides a sealed surface map of the study area (fig. 1). This map was used as input layer for deriving morphological information for each urban block.

Built-up density is an important indicator of urban structure that can readily be derived for each block from the sealed surface map as a spatial average. The resulting density map (fig. 2)

clearly shows the urban gradient from a compact and dense city centre to a low density, sprawled suburban zone with new residential developments to the northwest (Clonsilla, Hartstown, Tyrrelstown). While sealed surface density is easy to compute, it does not allow distinguishing between different land uses found within the area.

4.3 Characterising urban morphology

The frequency distribution of per-pixel sealed surface fractions, on the other hand, proves to provide important clues on a block's morphology and its functional use (fig. 3). As could be expected, low and medium density residential blocks contain more mixed sealed surface/vegetation pixels than industrial areas. The abundance of these mixed pixels is reflected by a sigmoid shaped cumulative frequency distribution (CFD), whereas the predominance of pure sealed surface pixels in industrial areas results in a more exponentially shaped CFD.

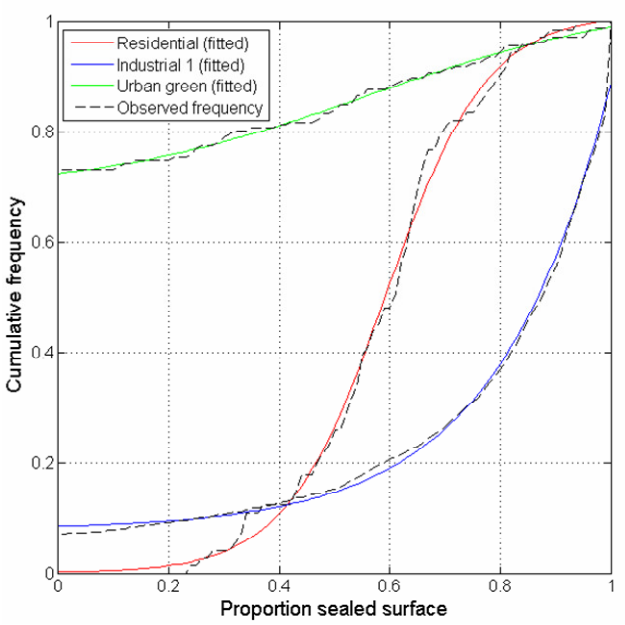

Figure 3. Cumulative frequency distribution of per-pixel sealed surface proportions and fitted logistic functions for a discontinuous residential block (red), an industrial zone (blue) and an urban green area (green).

The offset of the curves on the vertical axis indicates the presence of pure vegetation pixels, which in turn may point to vacant plots covered by grass within, for instance, an industrial zone. Blocks with little or no built-up areas are represented by a line close to the top of the unit square bounding the graph.
Fitting a transformed logistic function (equation (3)) to the observed frequency distribution provides 4 numerical parameters (table 1). Together, these parameters represent the frequency distribution of pixels with different amounts of sealed surface cover within the blocks, and as such may provide information that is helpful to discriminate between different land-use classes. For the example of the residential area shown in fig. 2, the block has a value of γ (scaling y-axis) close to 1 and a value of δ (translation y-axis) near 0, while the value of α is close to minus two times the value of β, thus indicating that the position of the point of inflection lies close to the middle of the unit square. For the industrial area shown in fig. 2, only a part of the sigmoid function's left side is required to obtain an optimal fit. Consequently, the right hand side of the function is shifted outside the area of the unit square, which is reflected in the values of the parameters α and β. The location of the function's point of inflection thus reflects the distinct shapes of industrial versus residential land. For the sigmoid-shaped residential curve in fig. 3, the point of inflection lies at [0.59;0.51]. For the more exponentially shaped industrial curve, it is located outside the graph's area at [2.07;80.57]. Also for the CFD of the industrial area shown in fig. 2, the value for the offset different from zero indicates that part the block's area is covered with pure vegetation pixels, vacant plots covered with grass in this case. Indeed, an offset value of 0.09 implies that 9% of the pixels within this block are pure vegetation pixels. The green curve near the top of the graph in fig. 2 represents an urban park that consists for 72% of pure vegetation pixels and contains only a small amount of mixed pixels.

	α	β	γ	δ	I_x	I_y	Offset
Residential	11.0	-6.5	1.0	0.0	0.6	0.5	0.0
Industrial	5.0	-10.3	161.0	0.1	2.1	80.6	0.1
Urban Green	4.0	-2.3	0.4	0.7	0.6	0.9	0.7

Table 1 Function parameters and derived parameters of some typical land use classes

4.4 Relating urban morphology to urban land use

To obtain a map characterising urban morphology and land use, the 4 CFD parameters were used in combination with average per-block sealed surface cover and spatial variance in a supervised classification strategy. The MLP classification produces an overall accuracy of 72% if 5 classes need to be identified (table 2). Especially the classes "commercial areas" and "services" have a low accuracy due the high degree of confusion. A classification with three classes (residential, non-residential, urban green) provides an acceptable overall accuracy of 86% .

MOLAND land use class	5 classes UA|PA		3 classes UA|PA	
Residential	82.39%	73.17%	80.41%	78.63%
Industrial	79.12%	87.76%		
Commercial	28.73%	22.43%	95.43%	88.93%
Services	55.90%	45.81%		
Green	67.65%	73.50%	62.69%	82.87%
Overall accuracy	71.98%		86.15%	

Table 2 User's accuracy (UA), producer's accuracy (PA) and overall accuracy of urban land use classification

The result of the MLP land-use classification with all variables, intersected with the urban density map (fig. 4), represents the

urban structure of Dublin rather well. Most misclassification between residential and non-residential areas occurs near the dense urban centre. This is related to the smaller block sizes in that area, which makes the frequency distribution of sealed surface proportions less reliable, and to the higher building density near the centre. The critical scale at which the analysis becomes less reliable will depend on the ratio between block size, image resolution and size of urban objects important for structural analysis

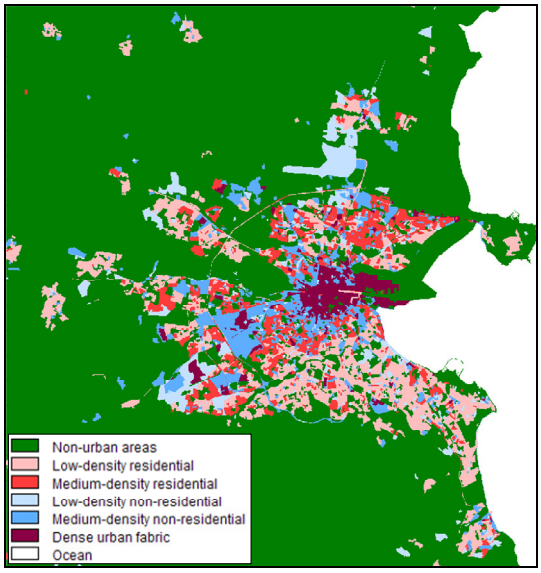

Figure 4. Morphological/functional map of Dublin derived from the Landsat image

5. CONCLUSION

Maps of urban morphology or structure are useful to urban planners and are especially valuable as input for calibrating urban land-use change models. The aim of this study was to characterise urban morphology inside predefined spatial regions using medium resolution remote sensing data. This type of data is available since the 1970's and allows composing the extensive time-series required for model calibration. In this paper we proposed a method to describe structure based on per-pixel sealed surface proportions within each region. These proportions were obtained by spectral unmixing of the satellite data. Three types of metrics were used to characterise the composition and spatial distribution of sealed surfaces within the regions: average sealed surface cover, spatial variance and the shape of the cumulative frequency distribution of the sealed surface proportions described by fitting a transformed logistic function. This approach showed promising results when applied to distinguish general morphological/functional land-use types such as residential versus non-residential land (industrial/ commercial/services). The distinction among the two functional classes residential/employment is important in the context of urban growth models because they represent the "push" and "pull" factors driving urban land-use change. The results of this study are currently being used to improve the calibration of the MOLAND urban growth model of the Greater Dublin Area. Future research should focus on determining optimal scales of analysis in relation to block size and image resolution.

6. REFERENCES

Atkinson, P.M., Tatnall, A.R.L., 1997. Neural Networks in Remote Sensing. *Int. J. Remote Sens.*, 18, pp. 699-709.

Bauer, M.E., Loffelholz, B.C., Wilson, B., 2008. Estimating and mapping impervious surface area by regression analysis of Landsat imagery. In: *Remote Sensing of Impervious Surfaces*, Weng, Q., Ed. CRC Press, Taylor & Francis Group, Boca Raton, pp. 3-19.

Cracknell, A.P.,1998. Synergy in remote sensing – what's in a pixel? *Int. J. Remote Sens.*, 19, pp. 2025-2047.

European Environment Agency (EAA), 2006. *Urban sprawl in Europe – the ignored challenge*. EAA report 10/2006, OPOCE , Luxemburg.

Herold, M., Couclelis, H., Clarke, K.C, 2005. The role of spatial metrics in the analysis and modelling of urban land use change. *Comput. Environ. Urban* , 29, pp. 369-399.

R.R. Irish, 2007. *Landsat 7 Science Data Users Handbook*. NASA, Greenbelt, MD, USA.

Ji, W, Ma, J., Twibell, R., Underhill, K., 2006. Characterising urban sprawl using multi-stage remote sensing images and landscape metrics. *Comput. Environ. Urban*, 30, pp. 861-879.

Martine, G., 2007. *The State of the World Population 2007*. United Nations Population Fund, New York, pp. 1.

Rashed, T., Weeks, J.R., Gadella, M.S., Hill, A.G., 2001. Revealing the anatomy of cities through spectral mixture analysis of multi-spectral satellite imagery: a case study of the Greater Cairo Region, Egypt, *Geocarto Int.*, 16, pp. 5-15.

van der Meer, F., 1999 Image classification through spectral unmixing. In: *Spatial Statistics for Remote Sensing*, A. Stein, F. van der Meer, B. Gorte, Eds. Kluwer Academic Publishers, Dordrecht, pp. 185-193.

Van de Voorde, T., De Genst, W., Canters, F., 2007. Improving pixel-based VHR land-cover classifications of urban areas with post-classification techniques, *Photogramm. Eng. Remote Sens.*, 73, pp. 1017-1027.

Van de Voorde, T., De Roeck, T., Canters, F., 2009. A comparison of two spectral mixture modelling approaches for impervious surface mapping in urban areas. *Int. J. Remote Sens*, 30, pp.4785 - 4806.

Ward, D., Phinn, S.R., Murray, A.T., 2000. Monitoring growth in rapidly urbanizing areas using remotely sensed data. *Professional Geogr.*, 52, pp. 371–385.

Weng, Q., 2008 *Remote Sensing of Impervious Surfaces*, CRC Press, Taylor & Francis Group, Boca Raton, FL, USA.

7. ACKNOWLEDGEMENTS

The research presented in this paper was supported by the Belgian Science Policy Office in the frame of the STEREO II programme - project SR/00/105. Marc Binard of the University of Liège is gratefully acknowledged for providing the high resolution land-cover classification.